Full Paper

CSIRO PUBLISHING

Aust. J. Chem. **2011**, *64*, 294–301

www.publish.csiro.au/journals/ajc

Self-ordering Electrochemistry: A Simple Approach for Engineering Nanopore and Nanotube Arrays for Emerging Applications*

Dusan Losic,[A,C] *Leonara Velleman,*[B] *Krishna Kant,*[A] *Tushar Kumeria,*[A] *Karan Gulati,*[A] *Joe G. Shapter,*[B] *David A. Beattie,*[A] *and Spomenka Simovic*[A]

[A]University of South Australia, Ian Wark Research Institute, Mawson Lakes Campus, Mawson Lakes, Adelaide, SA 5095, Australia.

[B]Flinders University, School of Chemical and Physical Science, Bedford Park, Adelaide, SA 5042, Australia.

[C]Corresponding author. Email: dusan.losic@unisa.edu.au

In this paper, we present recent work from our group focussed on the fabrication of nanopore and nanotube arrays using self-ordered electrochemistry, and their application in several key areas including template synthesis, molecular separation, optical sensing, and drug delivery. We have fabricated nanoporous anodic aluminium oxide (AAO) with controlled pore dimensions (20–200 nm) and shapes, and used them as templates for the preparation of gold nanorod/nanotube arrays and gold nanotube membranes with characteristic properties such as surface enhanced Raman scattering and selective molecular transport. The application of AAO nanopores as a sensing platform for reflective interferometric detection is demonstrated. Finally, a drug release study on fabricated titania nanotubes confirms their potential for implantable drug delivery applications.

Manuscript received: 31 October 2010.
Manuscript accepted: 23 December 2010.

Introduction

A fascinating number of new materials with nanoscale dimensions and different shapes and geometries have been generated in the past few decades and applied in numerous applications ranging from fundamental research, to development of new devices, to solving energy, environmental and medical problems.[1] Structures in the form of nanochannels, often defined as nanopores or nanotubes, are of particular interest where their functionality is directly influenced by the 1D-nanoscale nature of the geometry. These structures offer unique transport (ion, molecules, charge, energy), electrical, electrochemical, optical, and mechanical properties.[2] Therefore, it is not surprising that nanopores are widely employed in nature as key building blocks in some of the most sophisticated systems in living organisms (e.g. cell membranes).[3] Several approaches have been explored to fabricate materials with nanopore and nanotube structures, including focussed ion beam lithography, sol gel, phase separation, radiation etching, template, and electrochemical synthesis.[4–9]

Self-assembly, or the spontaneous organization of small units into large scale ordered and stable structures, is ubiquitous in nature and spans a wide range of scales. This concept, when used as a synthetic process, provides a cost effective and elegant route in nanotechnology for the spontaneous generation, ordering, and hierarchical organization of complex and functional nanomaterials at the molecular and nanoscale.[10] An analogous process described as self-ordering growth happens during the electrochemical anodization of selected metals where highly ordered arrays of nanopore and nanotube structures can be generated as a result of two competitive and continuous processes, one is oxide dissolution at the electrolyte/oxide interface, and the other is oxidation of metal at the oxide/metal interface.[9] This porous oxide growth on a metal surface (Scheme 1a) can be described as a close-packed hexagonal and perpendicular oriented array of columnar cells of oxide, each containing a central pore in which the size, length, and interval can be controlled by changing the anodization conditions.[11–13] Because the method is simple, inexpensive, lithography-free, and allows top-down fabrication using bulk metals with nanoscale precision, it is currently the most attractive nanofabrication approach.[6,14] However, the major disadvantage of this method is that it can be applied to a limited number of metals and alloys (Al, Ti, Nb, Ta, Hf, Si, W, Zr, TiAl, TiAlNb, TiZr, TiNb).[9] The two most commonly explored materials fabricated by this process are nanoporous anodic aluminium oxide (AAO) and titania nanotubes (TNT) with thousand publications appearing in the past several years.[9,15] In addition to their inexpensive and simple fabrication, these two materials offer many outstanding properties including: highly ordered and controllable structures, high surface area, high pore/tube aspect ratio,

*This is an invited contribution resulting from an oral presentation at RACI2010 (the Royal Australian Chemical Institute's National Convention), 4–8 July 2010, Melbourne.

10.1071/CH10398 0004-9425/11/030294

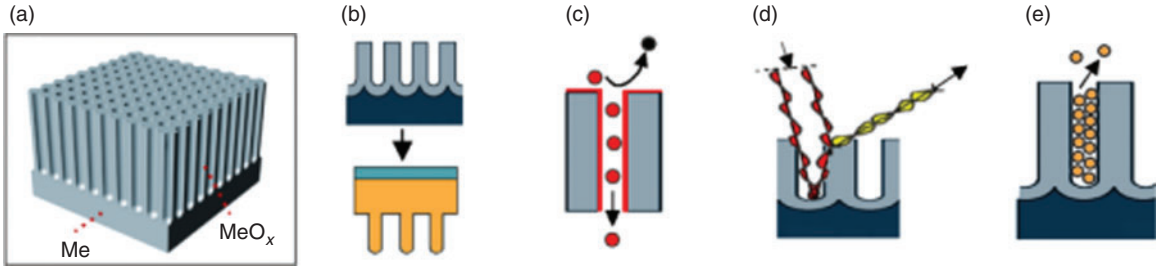

Scheme 1. (a) Scheme of metal oxide (MeO_x) pore structures formed by self-ordering electrochemical anodization of metal (Me), (b) scheme of template synthesis and transforming of nanopore into nanorod structures, (c) scheme of selective transport through chemically modified pores, (d) scheme of interferometric sensing by nanopores, and (e) scheme of drug delivery from nanotube implants.

photonic and optical properties, easy surface modification, chemical and thermal stability, biocompatibility, large band-gap (TNT only), and catalytic and self-cleaning properties (TNT only).[9,15–18]

The purpose of this paper in the special issue of the *Australian Journal of Chemistry* for the RACI 2010 conference is to present in a single publication selected research topics on the fabrication of AAO and TNT using a self-ordering electrochemistry approach, and their practical applications towards template synthesis of new nanomaterials and the development of devices for molecular separation, biosensing and drug delivery (Scheme 1b–e).

Results and Discussion

Controlling Pore Dimensions and Pore Geometries of AAO

To achieve a self-ordering regime and long-range ordered AAO pore structures with desired pore diameters, several growth regimes using conventional so called mild anodization (MA) and hard anodization (HA) in three common electrolytes, namely sulfuric acid, oxalic acid, and phosphoric acid, have been reported.[12,13,19] For complete control of fabrication there are numerous parameters that influence the anodization process which should be taken into consideration, including electrolyte concentration, chemical composition of electrolyte, voltage, current density, temperature, time, number of anodization steps and surface conditions (roughness, pre-patterning).[12,13,19–21] The selection of anodization conditions depends on required pore dimensions, porosity, and pore thickness. In our laboratory, we have developed a fully computer controlled anodization process using several fabrication conditions in MA and HA mode in both potentiostatic and galvanostatic mode using different electrolyte solutions, which allows the reproducible fabrication of AAO with controlled pore diameters (20 nm to 250 nm), porosity and thicknesses (<1 to >500 μm).[22,23] SEM images showing typical AAO structures with three different pore diameters fabricated in sulfuric acid at 25 V, oxalic acid at 40 V, and phosphoric acid at 195 V are presented in Fig. 1a–c.

Previous studies on AAO fabrication have focussed on the fabrication of AAO with straight, cylindrical pore structures.[12,13,20,21] To engineer more complex pore geometries, we recently developed a new anodization process, termed cyclic anodization.[24] The cyclic anodization concept is based on slow and oscillatory changes of anodization conditions that combines MA and HA and allows a periodic change in the growth process and pore diameters. It was demonstrated that by applying periodic oscillatory current signals during anodization, with different profiles, amplitudes, and periods, it is possible to perform structural modulation of AAO and control the geometry of pore structures.[24] AAO with asymmetrical (ratchet-type) and symmetrical (circular) pore geometries, with different lengths, periodicity, and gradients were fabricated by changing the profile of the current signal, amplitude, and period. By using multi-profiled current signals during anodization we demonstrated that it is possible to perform nanosculpturing of AAO with distinctive, hierarchical pore structures with different periodicity and shapes.[24,25] Several examples of AAO with uniform and asymmetrical periodicity of modulated pore structures fabricated under the galvanostatic mode in phosphoric acid using asymmetrical cycling signal with current density 10–120 mA cm^{-2} and frequencies (0.5 min to 2 min) are shown in Fig. 1d–f. Images show that the length and the shape of periodic pore structures can be controlled by the amplitude and frequency of the cyclic signal.

Template Synthesis of Gold Nanorod and Periodically Shaped Nanotube Arrays Using AAO Templates

Nanopore/nanotube array materials that have fine, uniform channels of nanometre dimensions, have stimulated considerable interest in recent years due to their utilization as a host or template structure for nanometre devices, such as magnetic, electronic, optoelectronic, electrochemical, separation, and drug delivery devices.[6,14,26,27] Hence, it is not surprising that template synthesis, using AAO, is currently one of the most popular synthetic methods offering very simple and inexpensive preparation of materials with nanoscale dimensions in many different forms such as particles, wires, rods, tips, and tubes and from different materials including metals, semiconductors, metal oxides, carbon nanotubes, and polymers.[6,26,28] In our group we are focussed on the development of methods for the fabrication of 1- and 2D nanorod and nanotube structures with periodically shaped geometries to advance their optical (localized surface plasmon resonance and surface enhanced Raman Spectroscopy/Scattering (SERS)), transport (molecular separation properties) and magnetic (targeting drug delivery) properties. We have developed several synthetic approaches including thermal evaporation, chemical and electrochemical deposition and chemical vapour deposition to grow metal, metal oxide, and carbon nanotube structures with different shapes and geometries using AAO templates.

Fig. 2a and b shows SEM images of gold film arrays with highly ordered nanorod structures fabricated by the simple process of evaporation of gold onto the AAO template. The AAO template was prepared by three anodization steps in oxalic acid (0.3 M), at 50 V and 0°C in order to obtain highly ordered pore structures with pore lengths shorter than 1 μm. The size of gold structures (from 20 to 200 nm) and their aspect ratio (1 to 50) can be controlled by the dimensions of the AAO pores by selecting appropriate anodization conditions.[29] Therefore, through this method it is possible to control the plasmonic

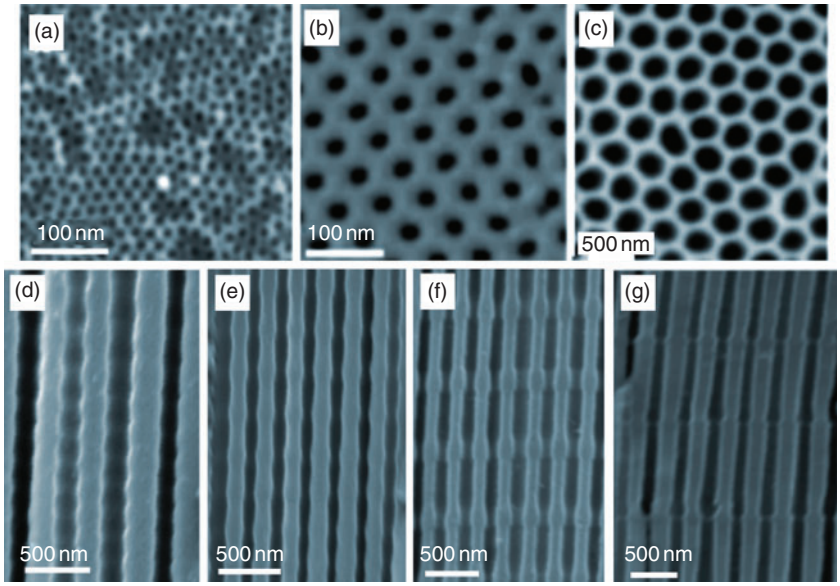

Fig. 1. Pore structures of anodic aluminium oxide (AAO) prepared by anodization of Al foil using different conditions (a) 0.1 M sulfuric acid at 25 V, (b) 0.3 M oxalic acid at 40 V, and (c) 0.3 M phosphoric acid at 195 V. (d–g) AAO with periodically shaped pore structures using cyclic anodization in 0.1 M phosphoric acid using continuous cycle with different profiles (saw tooth, sinusoidal) and amplitudes $I_{min} = 10$ mA to $I_{max} = 120$ mA and periods 0.2–2 min.

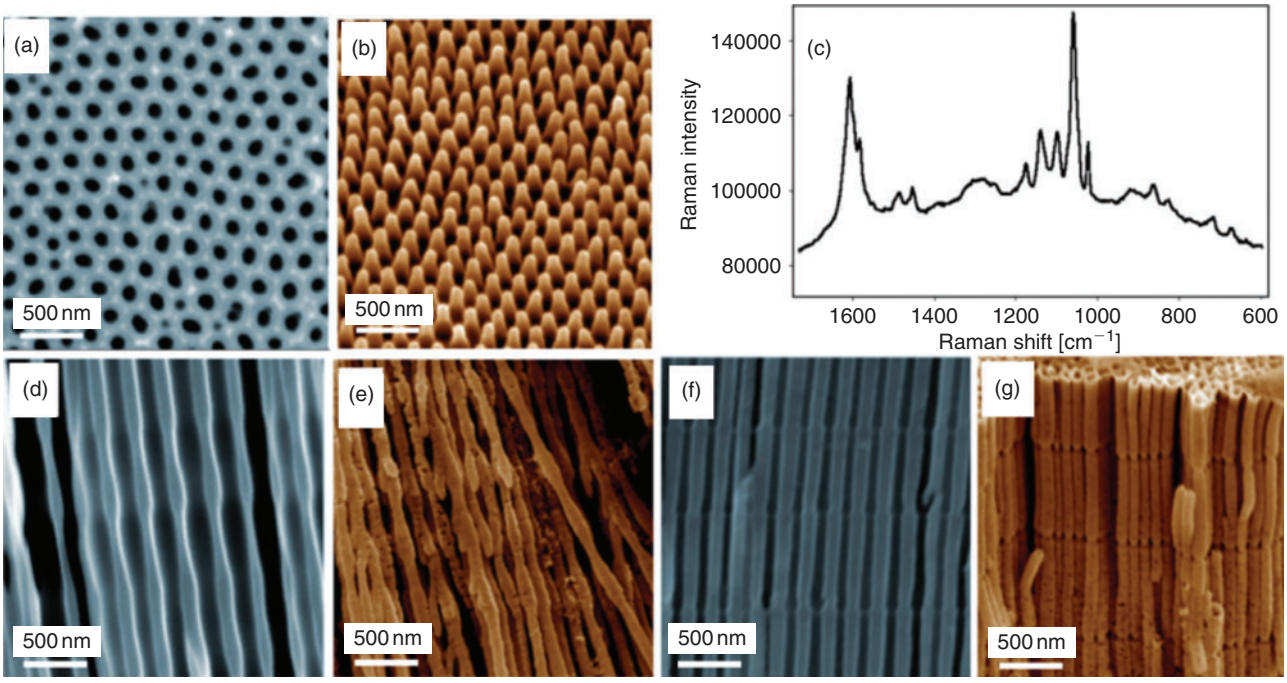

Fig. 2. (a, b) SEM images of AAO template with nanopores and corresponding gold nanoarrays formed by thermal deposition of gold followed by removal of the template. (c) A typical SERS spectrum collected from gold nanorod structures immersed in 0.001 M thiosalicylic acid as a model SERS probe molecule. (d–g) SEM image of gold nanotube and nanorod structures with periodically shaped geometries prepared by template synthesis using electroless deposition of gold inside of AAO.

properties of these gold nanostructures for specific sensing applications.[29] We evaluated the performance of the prepared gold nanorod structures as a SERS gold substrate using immersion in a 0.001 M thiosalicylic acid (a model SERS probe molecule) solution. Fig. 2c shows a typical SERS spectrum acquired in extended continuous scanning mode (60 s exposure at each wave number), with a 633 nm HeNe laser and a ×50 objective lens using a commercial Raman microscope (Renishaw System 1000, UK). A large enhancement in the Raman signal in comparison with a smooth gold surface is observed ($>10^5$ times), which demonstrates the feasibility of these structures to be used as a SERS active substrate for the chemical detection of adsorbed molecules.[30,31] These gold nanorod films can be fabricated with different patterns and large areas (e.g. 5 cm × 5 cm), only limited by the size of the original AAO template, offering a solution for inexpensive fabrication

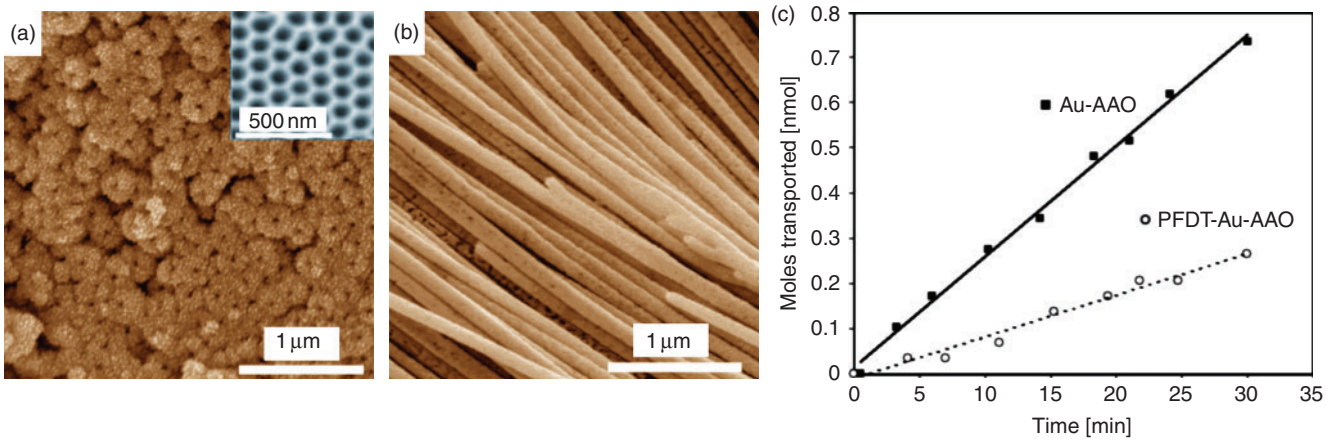

Fig. 3. (a) SEM image showing the surface morphology of gold nanotube membranes (Au-AAO) fabricated by gold electroless deposition on an AAO membrane with a pore diameter of 80 nm. Inset: uncoated porous AAO membrane. (b) Liberated gold nanotubes after dissolution of the AAO template. (c) Transport of a hydrophilic dye (EY) across an unmodified and hydrophobic (PFDT) modified Au-PA membrane.

Table 1. Transport and selectivity properties of bare and chemically functionalized gold nanotube membranes (Au-AAO)

Error bar ± SD of three measurements

Membrane	Flux of permeate molecule [mol $cm^{-2} h^{-1}$]		Flux ratio
	Rubpy	EY	Rubpy:EY
Au-AAO (bare)	$3.50 \pm 0.08 \times 10^{-7}$	$6.40 \pm 0.61 \times 10^{-8}$	5.47
PFDT/Au-AAO	$3.29 \pm 0.19 \times 10^{-7}$	$2.23 \pm 0.06 \times 10^{-8}$	14.76

of sensing platforms for SERS or localized surface plasmon resonance biosensing devices. One limitation of the direct metal deposition method is the fabrication of structures with higher aspect ratios (>50) because thermal metal deposition inside deeper pores (>2 µm) is restricted. To prepare films with a higher aspect ratio for gold nanostructures, a different metal deposition method is required if one is to perform conformal deposition inside of pores such as electrochemical.

Modelling studies predict that nanorods and nanotubes with periodically structured or shaped structures could offer unique optical, magnetic, electrical, and transport properties but their fabrication is still a challenging problem.[32] We have shown that by using AAO templates with shaped pore structures, it is possible to design nanowires and nanotubes with very complex architectures and therefore achieve many of these unique, but still unexplored properties. Fig. 2d–g shows examples of gold nanotube structures with periodically shaped geometry fabricated using these AAO templates. AAO templates were prepared by cyclic anodization in phosphoric acid 0.1 M using the galvanostatic mode followed by electroless deposition of gold. By coupling AAO templates with different pore shapes and different deposition methods we have demonstrated fabrication of very complex nanotube structures of Ni and carbon nanotubes and the exploration of their magnetic and electrical properties is currently under investigation.

Chemically Selective Molecular Transport with Functionalized Gold Nanotube Membranes

Gold nanotube membranes were prepared by electroless deposition of gold within the pores of AAO templates (Au-AAO) using previously described methods.[33,34] AAO membranes are an ideal platform to investigate the fundamentals of transport phenomena due to their uniform cylindrical pores and narrow pore size distribution. The electroless deposition of gold allows the precise reduction of the pore diameters of the Au-AAO membrane (Fig. 3a) in comparison with the uncoated AAO membrane (Fig. 3a, inset), with pore diameters being decreased to ~15 nm. In order to verify that gold deposition has occurred within the pores of the membrane and to ensure deposition extends through the entire length of the pore, the AAO template was dissolved to reveal an array of gold nanotubes (Fig. 3b). In addition, the gold provides a platform for further surface functionalization using self assembled monolayers, therefore providing an ideal model for studying how surface chemistry affects the transport properties of the membrane.[34,35] The immobilization of appropriate functional groups on the membrane surface allows for selective transport of permeate molecules.[36,37] The effect of surface chemistry on the selectivity and transport properties of fabricated gold nanotube membranes has been demonstrated through functionalization with highly hydrophobic thiol (1*H*,1*H*,2*H*,2*H*-perfluorodecanethiol, PFDT). The flux of a hydrophobic dye tris(2,2′-bipyridyl)dichlororuthenium(II) hexahydrate (Rubpy) and a hydrophilic dye Eosin Yellow (EY) were measured through PFDT-Au-AAO membranes and is presented in Fig. 3c and Table 1. The transport rates of the hydrophobic dye remain relatively constant after PFDT modification. This indicates that the incorporation of a hydrophobic thiol does not hinder the transport of hydrophobic species. Fig. 3c presents the transport of EY though the Au-AAO membrane before and after surface modification with PFDT. The transport of the hydrophilic dye has been decreased significantly with the addition of the hydrophobic monolayer onto the membrane. The flux ratio

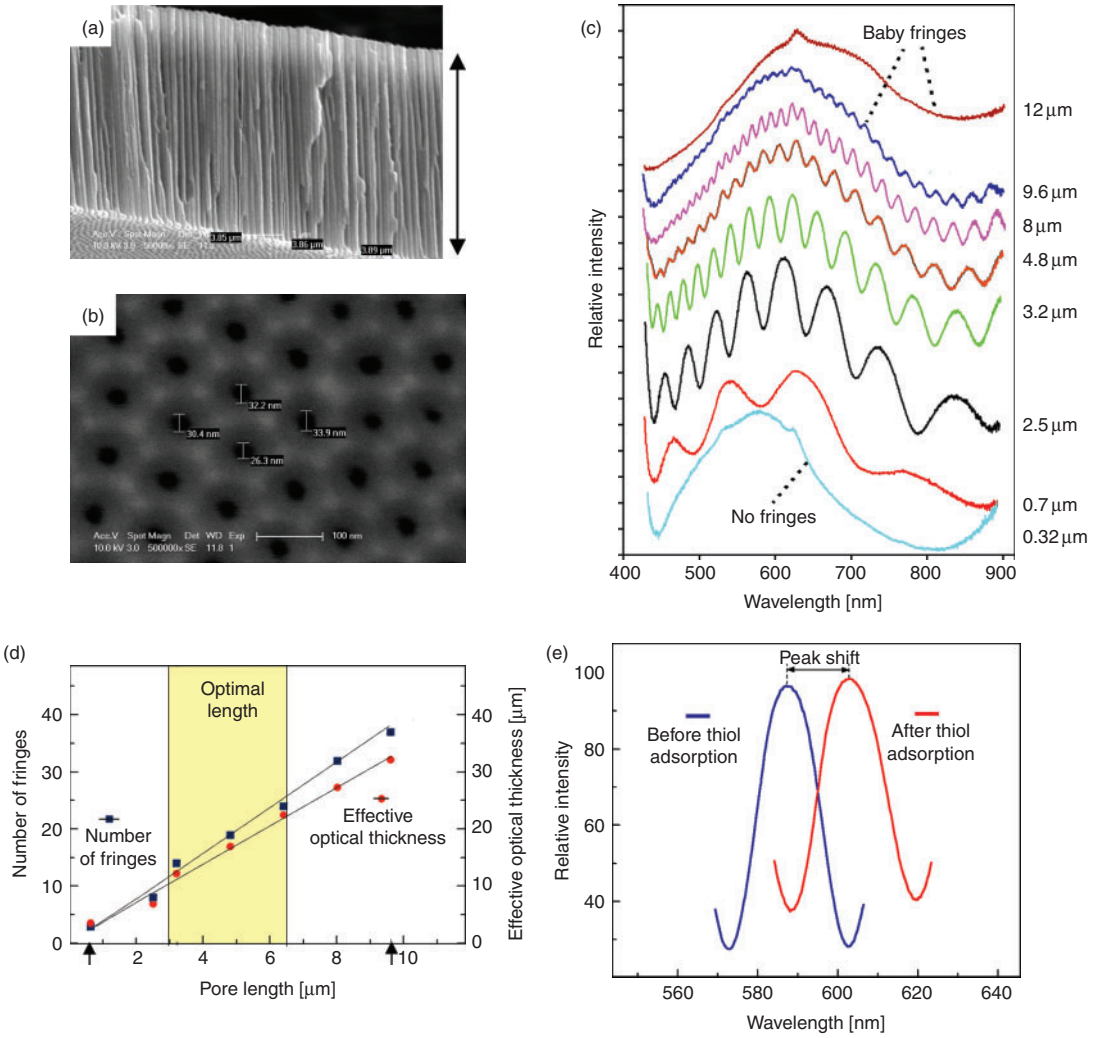

Fig. 4. (a, b) SEM image of AAO cross-section and the top pore surface, (c) series of reflective interference spectra from AAO pores with pore length from 0.3 µm to 12 µm, (d) influence of number of fringes and optical thickness of pore length, and (e) a typical interoferometric signal of an optimized AAO sensor modified with gold film (10 nm) showing the shift of fringe signal as a result of adsorption of 0.01 M thiosalicylic acid on gold.

(Table 1) describes the degree of separation of the two dyes through each of the membranes. After PFDT modification, the flux ratio is increased by 170% illustrating the improvement in the selectivity of the membrane towards the transport of hydrophobic species while rejecting hydrophilic species. The future of this separation approach, on which we are currently working, lies in developing 'switchable' membranes that can function in a highly controllable manner.

Optimization of Optical Properties of Nanopores Towards the Development of an AAO Label Free Interferometric Biosensor

Reflective interference spectroscopy is a sensitive optical method based on white light interference in a thin film where the interference pattern depends on the product of refractive index (n) and thickness (L), nL.[38] The binding of analyte to the surface of the thin film produces an increase in the film thickness (L), which results in a shift in the interference pattern measured in the optical spectrum. The employment of a porous thin film to increase the surface area for analyte capture is shown to have a significant impact on the sensitivity of the interferometric sensor.[39] Therefore, it is not surprising that porous silicon is demonstrated to be an effective optical interferometric sensing material due to its large surface area.[38,40] However, porous silicon has a considerable limitation due to its poor stability and rapid degradation, which can significantly influence the biosensing signal. To address this problem, a porous film based on AAO and TNT has recently been demonstrated as a new alternative towards the development of more stable interferometric biosensing devices.[41,42]

To optimize the interferometric signal from AAO pores for biosensing applications we investigated the influence of several parameters including: pore diameter; pore interdistance; pore length; and the external and internal modification of pore structures. In this work, we present how the interferometric signal can be tuned by the length of the pore structures prepared using different anodization conditions. Fig. 4a and b shows the typical cross-section and the top surface of AAO pore structure prepared by electrochemical anodization in oxalic acid (voltage 50 V and anodization time 20 min, temperature 0°C). The influence of the pore lengths (from 0.3 to 12 µm) prepared using different conditions (voltage 60 V and anodization times from 5 to 30 min) on the interference pattern (Fabry–Perot fringes) signal is shown in Fig. 4c and d. These results demonstrate that the number of fringes increases with increasing pore length and the graph shows that there is a critical range of pore length

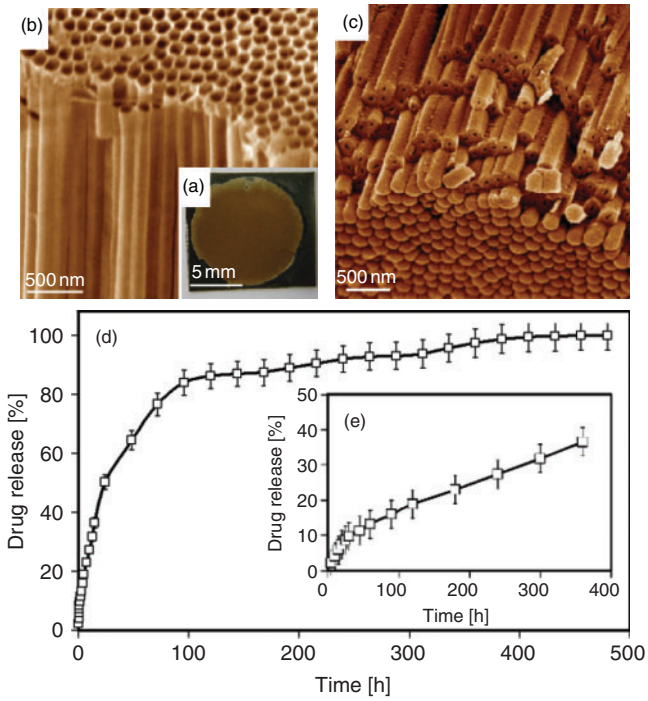

Fig. 5. (a) Whole titania nanotube (TNT) implant on Ti foil, (b, c) SEM images of detached TNT showing cross-sectional nanotube structure with closed tubes on the bottom, (d, e) drug release of indomethacin from TNT showing burst (the first 6 h) and slow release (over 20 days).

(>0.5 μm and <10 μm). Pores with lengths outside this range cannot produce analytically useful interference fringe signals. The optimal pore length of AAO to produce a good interference signal with an optimal number of fringes and high frequency is between 3 and 6.5 μm. These results confirm that pore length has a significant influence on the interference signal, which requires careful consideration during the fabrication of AAO interference sensors. A typical interoferometric signal of an optimized AAO sensor modified with gold film (10 nm) showing a shift of fringe signal as a result of adsorption of 0.01 M thiosalicylic acid on gold surface is presented in Fig. 4e. A large shift of interference signal (>20 nm) is observed even when a very low concentration was used (0.0001 M) showing excellent sensitivity and applicability of the AAO pore platform as an interferometric biosensing device. We are currently working to expand the sensing and biosensing capabilities of AAO nanopore platforms for practical applications.

TNT for Implantable Drug Delivery Applications

Highly ordered and vertically aligned pores and nanotubular structures fabricated by self-ordering electrochemical processes of biocompatible metals and their alloys such as Ti, Ta, Al, W, are recognized as an attractive solution for the design of implantable drug delivery systems for coronary stents, bones, and tissue engineering.[9,17,27,43,44] Their attractiveness is based on controllable dimensions of pore/nanotube structures, tailored surface chemistry, high surface area, high drug loading capability, chemical stability, biocompatibility, low cost, simple, and scalable fabrication.[9,27] Here we present the drug loading and release characteristics of TNT films using an anti-inflammatory drug (indomethacin) to prove their potential application as bone implants for the delivery of therapeutics to prevent infections and ensure better acceptance of the implant in bones.

A TNT layer with a diameter of 1 cm formed on titanium foil by the anodization process is shown in Fig. 5a. The typical morphology of the prepared nanotube structures was confirmed by SEM, and is summarized in Fig. 5b and c, which shows a cross-section and the top and bottom surfaces. By controlling the anodization voltage (60–100 V) it is possible to control the nanotube diameters from 70–90 nm to 150–180 nm.[9] The nanotube growth rate also shows a similar linear dependence with the anodization voltage that is used to fabricate TNT with desired thicknesses (40 μm). The drug release kinetics monitored by UV spectroscopy show a burst release during the first 6 h of release (Fig. 5e). A slow and time delayed pattern in release was observed over the following 2–3 weeks (Fig. 5d). Similar release characteristics were observed using TNT formed on Ti wire. These results demonstrate that a large amount of drug can be loaded into TNT with release behaviour suitable for use in drug-release implants. To further extend release and achieve a sustained release pattern with zero order kinetics for more than 1 month, or achieve externally triggered drug release, we are exploring strategies using polymer modifications and magnetic nanoparticles.[45]

Conclusions

This paper highlights progress from our group towards developing self-ordering electrochemical approaches for the fabrication of materials with ordered nanopore and nanotube structures and their application into useful devices (separation, sensing, and drug delivery). The body of work presented has illustrated the many capabilities of nanopore and nanotube structures fabricated by this process based on the simple electrochemical anodization of aluminium and titanium foils. The fabrication process has been optimized to allow fabrication of AAO with controllable pore diameters and length. We have also demonstrated a new technique called cyclic anodization which allows for the controllable manipulation of nanopore geometry. We have shown that AAO can be used for the template synthesis of highly ordered gold nanorod films and gold nanotube arrays with periodically shaped geometries, and we are working to further explore their optical and transport properties. Template synthesis was also used to prepare gold nanotube membranes and these membranes were modified with self-assembled monolayers with specific functional groups to demonstrate the chemically selective separation of hydrophobic and hydrophilic molecules. The reflective interference properties of AAO nanopores were demonstrated and optimized showing the capability that AAO can serve as a suitable platform for the development of label-free interferometric biosensing devices. We are currently working to expand the biosensing capabilities of these structures. Finally, we have shown that TNT nanotube arrays fabricated by the anodization of Ti foil or wires can be used for the delivery of drugs with potential to be applied as implantable drug delivery devices for bone therapy. Results presented here suggest that self-ordering electrochemistry shows many advantages for the fabrication of nanopore and nanotube structures with great promise to be a benchmark for the development of many practical devices.

Experimental

Preparation of Porous AAO

A high purity (99.997%) aluminium foil supplied by Alfa Aesar (USA) was used for preparation of AAO by electrochemical anodization using previously described procedures.[20] Briefly,

the Al foil was cleaned in acetone and then electrochemically polished in a 1:4 volume mixture of perchloric acid/ethanol followed by a two step anodization process using different acids (0.1 M sulfuric acid at 25 V, 0.3 M oxalic acid at 40 V and 0.3 M phosphoric acid at 40 V) for the required time (10 min to 16 h). The anodization was performed using an electrochemical cell equipped with a cooling stage at a temperature of 0°C. To prepare periodically shaped AAO, cyclic anodization was performed using a computer controlled power supply (Agilent, USA) and specially developed LabView based software (National Instrument, USA).[24] Galvanostatic cyclic anodization in 0.1 M phosphoric acid was performed using continuous cycle with different profiles (saw tooth, sinusoidal), amplitudes ($I_{min} = 10$ mA to $I_{max} = 120$ mA), periods ($t = 0.2$–2 min), and number of cycles ($n = 10$–50).[24] After anodization, if required, the remaining Al layer was removed from the AAO films using $CuCl_2$/HCl solution. The free-standing AAO membrane was prepared by a pore opening process to remove a barrier layer on the bottom using 5% phosphoric acid for minimum 60–70 min.

Preparation of Nanotube Titania (TNT)

Titanium (Ti) foil and wires (99, 6%, Alfa Aesar), were mechanically polished and cleaned by sonication in acetone for 30 min before anodization. TNT film in the form of a porous layer on Ti foil (0.25 mm) and Ti wires (0.5 mm) was prepared by two anodization steps using NH_4F/ethyleneglycol electrolyte (3% water and 0.3% NH_4F) and a voltage of 100 V at 20°C for 2 h by a previously described procedure.[46,47] The drug (indomethacin, 0.012 g mL^{-1} in ethanol) was loaded on TNT via consecutive deposition (20 times) followed by drying under vacuum for 2 h.[45]

Template Synthesis of Gold Nanorod and Nanotube Arrays and Nanotube Membrane

Cold film with nanorod arrays was prepared by thermal deposition of gold on AAO template by adapting our method developed for preparation of ultra-flat gold film.[48,49] The AAO template was prepared with a three step anodization process of Al foil using 0.3 M oxalic acid, 40 V at 0°C, and 10–20 min anodization time in order to achieve ordered pores with short lengths. The gold electroless plating method was used to coat internal pores of AAO template to prepare gold nanotube (Au-AAO) arrays and gold nanotube membranes. For the preparation of gold nanotubes with periodically shaped structures, AAO with shaped pores was used as the template. This template was prepared by cyclic anodization using the procedure described in the previous section. We used the electroless gold deposition process described by Martin et al. and refined by our group.[33,34] Electroless deposition consists of several steps; sensitization of the membrane with tin ($SnCl_2$, 0.026 M), activation with silver ($AgNO_3$, 0.035 M) and the deposition of gold ($Na_3Au(SO_3)_2$, 7.9×10^{-3} M). Au-AAO membranes were functionalized with thiol 1*H*,1*H*,2*H*,2*H*-perfluorodecanethiol (PFDT) by immersion in 1 mM PFDT solution in ethanol for 48 h, followed by rinsing in ethanol and drying in air. This procedure results in a monolayer of PFDT over the gold surfaces inside of pores of the membrane.

Structural and Functional Characterizations

The scanning electron microscope (SEM) images of prepared samples were obtained by Philips XL-30 and FIB Helios Nanolab 600 (FEI Co.).

The SERS spectrum from gold nanorod film was collected using a commercial Raman microscope (Renishaw System 1000, UK). The spectrum was acquired in extended continuous scanning mode (60 s exposure at each wave number), using a 633 nm HeNe laser (power ~5 mW at sample) and a ×50 objective lens. The Raman light was separated from the laser line using a notch filter and the Raman spectrum dispersed onto a Peltier cooled CCD detector.

Transport experiments were performed using a U-tube permeation cell in which the membrane separates two half-cells; the feed cell and the permeate cell. The hydrophobic dye, tris(2,2′-bipyridyl)dichlororuthenium(II) hexahydrate (Rubpy), and the hydrophilic dye, EY, were used to probe the transport properties of the membranes.[34,37] Separate permeation experiments were performed with Rubpy and EY in which a 1 mM solution of the dye in water was added to the feed cell and water was added to the permeate cell. The diffusion of the dye from the feed cell to the permeate cell was continuously monitored with a UV-Vis fibre optic spectrophotometer (Ocean Optics, USA) at 286 nm (Rubpy) and 517 nm (EY).

The reflective interferometric study of the prepared AAO with different pore lengths and pore diameters was performed by Ocean Optics spectrometer, and film thickness monitor Filmetrics 20. Fast Fourier Transform was applied on the collected data to get effective optical thickness using IGOR Pro (Wavemetrics).

The amount of drug (indomethacin) loaded on TNT was determined by thermogravimetric analysis (Q Series™ Thermal Analysis, Universal Analysis 2000). Loaded samples were heated from 20 to 600°C at a scanning rate of 10°C min^{-1} in nitrogen.

The release characteristic of TNT loaded with drug was determined by placing implant in phosphate buffer and monitoring absorbance at 319 nm by UV–visible spectrophotometer (Cary 1) at different time intervals from every 5–10 min during first 6 h and then every day for 2 weeks.

Acknowledgements

This work is supported by the Australian Research Council (DP 0770930, DP 1096282, and LP 100100272) and the University of South Australia. We thank the Australian Microscopy and Microanalysis Research Facility (AMMRF), South Australian Node for use of the microscopy facility.

References

[1] S. Mann, G. A. Ozin, *Nature* **1996**, *382*, 313. doi:10.1038/382313A0
[2] R. W. Murray, *Chem. Rev.* **2008**, *108*, 2688. doi:10.1021/CR068077E
[3] C. R. Martin, Z. S. Siwy, *Science* **2007**, *317*, 331. doi:10.1126/SCIENCE.1146126
[4] M. Ulbricht, *Polymer* **2006**, *47*, 2217. doi:10.1016/J.POLYMER.2006.01.084
[5] C. C. Striemer, T. R. Gaborski, J. L. McGrath, P. M. Fauchet, *Nature* **2007**, *445*, 749. doi:10.1038/NATURE05532
[6] M. Steinhart, R. B. Wehrspohn, U. Gosele, J. H. Wendorff, *Angew. Chem. Int. Ed.* **2004**, *43*, 1334. doi:10.1002/ANIE.200300614
[7] W. Lee, M. Alexe, K. Nielsch, U. Gosele, *Chem. Mater.* **2005**, *17*, 3325. doi:10.1021/CM050480Z
[8] P. Apel, *Radiat. Meas.* **2001**, *34*, 559. doi:10.1016/S1350-4487(01)00228-1
[9] A. Ghicov, P. Schmuki, *Chem. Commun.* **2009**, 2791. doi:10.1039/B822726H
[10] H. Cölfen, S. Mann, *Angew. Chem. Int. Ed.* **2003**, *42*, 2350. doi:10.1002/ANIE.200200562
[11] J. W. Diggle, T. C. Downie, S. W. Goulding, *Chem. Rev.* **1969**, *69*, 365. doi:10.1021/CR60259A005

[12] O. Jessensky, F. Muller, U. Gosele, *Appl. Phys. Lett.* **1998**, *72*, 1173. doi:10.1063/1.121004
[13] W. Lee, R. Ji, U. Gosele, K. Nielsch, *Nat. Mater.* **2006**, *5*, 741. doi:10.1038/NMAT1717
[14] H. Chik, J. M. Xu, *Mater. Sci. Eng. Rep.* **2004**, *43*, 103. doi:10.1016/J.MSER.2003.12.001
[15] C. A. Grimes, *J. Mater. Chem.* **2007**, *17*, 1451. doi:10.1039/B701168G
[16] G. K. Mor, O. K. Varghese, M. Paulose, K. Shankar, C. A. Grimes, *Sol. Energy Mater. Sol. Cells* **2006**, *90*, 2011. doi:10.1016/J.SOLMAT.2006.04.007
[17] J. Park, S. Bauer, P. Schmuki, K. von der Mark, *Nano Lett.* **2009**, *9*, 3157. doi:10.1021/NL9013502
[18] P. Roy, D. Kim, I. Paramasivam, P. Schmuki, *Electrochem. Commun.* **2009**, *11*, 1001. doi:10.1016/J.ELECOM.2009.02.049
[19] H. Masuda, F. Hasegwa, S. Ono, *J. Electrochem. Soc.* **1997**, *144*, L127. doi:10.1149/1.1837634
[20] H. Masuda, K. Fukuda, *Science* **1995**, *268*, 1466. doi:10.1126/SCIENCE.268.5216.1466
[21] G. E. Thompson, *Thin Solid Films* **1997**, *297*, 192. doi:10.1016/S0040-6090(96)09440-0
[22] S. Ono, H. Asoh, M. Saito, M. Ishiguro, *Electrochemistry* **2003**, *71*, 105.
[23] M. Lillo, D. Losic, *J. Membr. Sci.* **2009**, *327*, 11. doi:10.1016/J.MEMSCI.2008.11.033
[24] D. Losic, M. Lillo, D. Losic, Jr, *Small* **2009**, *5*, 1392. doi:10.1002/SMLL.200801645
[25] D. Losic, D. Losic, Jr, *Langmuir* **2009**, *25*, 5426. doi:10.1021/LA804281V
[26] R. E. Sabzi, K. Kant, D. Losic, *Electrochim. Acta* **2010**, *55*, 1829. doi:10.1016/J.ELECTACTA.2009.10.075
[27] D. Losic, S. Simovic, *Expert Opin. Drug Deliv.* **2009**, *6*, 1363. doi:10.1517/17425240903300857
[28] Y. Piao, H. Lim, J. Y. Chang, W. Y. Lee, H. Kim, *Electrochim. Acta* **2005**, *50*, 2997. doi:10.1016/J.ELECTACTA.2004.12.043
[29] D. Losic, J. G. Shapter, J. G. Mitchell, N. H. Voelcker, *Nanotechnology* **2005**, *16*, 2275. doi:10.1088/0957-4484/16/10/049
[30] J. N. Anker, W. P. Hall, O. Lyandres, N. C. Shah, J. Zhao, R. P. Van Duyne, *Nat. Mater.* **2008**, *7*, 442. doi:10.1038/NMAT2162
[31] K. A. Willets, R. P. Van Duyne, *Annu. Rev. Phys. Chem.* **2007**, *58*, 267. doi:10.1146/ANNUREV.PHYSCHEM.58.032806.104607
[32] P. W. Bohn, *Annu. Rev. Anal. Chem.* **2009**, *2*, 279. doi:10.1146/ANNUREV-ANCHEM-060908-155130
[33] M. Nishizawa, V. P. Menon, C. R. Martin, *Science* **1995**, *268*, 700. doi:10.1126/SCIENCE.268.5211.700
[34] L. Velleman, J. G. Shapter, D. Losic, *J. Membr. Sci.* **2009**, *328*, 121. doi:10.1016/J.MEMSCI.2008.11.055
[35] A. M. M. Jani, E. J. Anglin, S. J. P. McInnes, D. Losic, J. G. Shapter, N. H. Voelcker, *Chem. Commun.* **2009**, 3062. doi:10.1039/B901745C
[36] C. R. Martin, M. Nishizawa, K. Jirage, M. S. Kang, S. B. Lee, *Adv. Mater.* **2001**, *13*, 1351. doi:10.1002/1521-4095(200109)13:18<1351::AID-ADMA1351>3.0.CO;2-W
[37] L. Velleman, G. Triani, P. J. Evans, J. G. Shapter, D. Losic, *Microporous Mesoporous Mater.* **2009**, *126*, 87. doi:10.1016/J.MICROMESO.2009.05.024
[38] V. S. Y. Lin, K. Motesharei, K. P. S. Dancil, M. J. Sailor, M. R. Ghadiri, *Science* **1997**, *278*, 840. doi:10.1126/SCIENCE.278.5339.840
[39] A. Janshoff, K. P. S. Dancil, C. Steinem, D. P. Greiner, V. S. Y. Lin, C. Gurtner, K. Motesharei, M. J. Sailor, M. R. Ghadiri, *J. Am. Chem. Soc.* **1998**, *120*, 12108. doi:10.1021/JA9826237
[40] K. S. Mun, S. D. Alvarez, W. Y. Choi, M. J. Sailor, *ACS Nano* **2010**, *4*, 2070. doi:10.1021/NN901312F
[41] S. D. Alvarez, C. P. Li, C. E. Chiang, I. K. Schuller, M. J. Sailor, *ACS Nano* **2009**, *3*, 3301. doi:10.1021/NN900825Q
[42] Y. Y. Song, H. Hildebrand, P. Schmuki, *Electrochem. Commun.* **2009**, *11*, 1429. doi:10.1016/J.ELECOM.2009.05.022
[43] K. C. Popat, M. Eltgroth, T. J. LaTempa, C. A. Grimes, T. A. Desai, *Biomaterials* **2007**, *28*, 4880. doi:10.1016/J.BIOMATERIALS.2007.07.037
[44] K. C. Popat, M. Eltgroth, T. J. La Tempa, C. A. Grimes, T. A. Desai, *Small* **2007**, *3*, 1878. doi:10.1002/SMLL.200700412
[45] S. Simovic, D. Losic, K. Vasilev, *Chem. Commun.* **2010**, *46*, 1317. doi:10.1039/B919840G
[46] K. Vasilev, Z. Poh, K. Kant, J. Chan, A. Michelmore, D. Losic, *Biomaterials* **2010**, *31*, 532. doi:10.1016/J.BIOMATERIALS.2009.09.074
[47] K. Kant, D. Losic, *Phys. Status Solidi RRL* **2009**, *3*, 139. doi:10.1002/PSSR.200903087
[48] D. Losic, J. G. Shapter, J. J. Gooding, *Aust. J. Chem.* **2001**, *54*, 643. doi:10.1071/CH01122
[49] J. Mazurkiewicz, F. J. Mearns, D. Losic, L. Weeks, E. R. Waclawik, C. T. Rogers, J. G. Shapter, J. J. Gooding, *J. Vac. Sci. Technol. B* **2002**, *20*, 2265. doi:10.1116/1.1518968